

Deep Learning-Based Plant Health State Classification Using Image Data

Ali Asgher Syed¹, Jaehawn Lee², Alvaro Fuentes^{3*}, Sook Yoon⁴, Dong Sun Park⁵

¹Master's Student, Department of Electronics Engineering, Jeonbuk National University

²Ph.D. Student, Department of Electronics Engineering, Jeonbuk National University

³Research Professor, Core Research Institute of Intelligent Robots, Jeonbuk National University

⁴Professor, Department of Computer Engineering, Mokpo National University

⁵Professor, Core Research Institute of Intelligent Robots, Jeonbuk National University

영상 데이터를 이용한 딥러닝 기반 작물 건강 상태 분류 연구

세이드 알리 에스거¹, 이재환², 알바로 푸엔테스^{3*}, 윤숙⁴, 박동선⁵

¹전북대학교 전자공학부 석사과정, ²전북대학교 전자공학부 박사과정, ³전북대학교 지능형로봇연구소 연구교수,

⁴목포대학교 컴퓨터공학과 교수, ⁵전북대학교 지능형로봇연구소 교수

Abstract Tomatoes are rich in nutrients like lycopene, β -carotene, and vitamin C. However, they often suffer from biological and environmental stressors, resulting in significant yield losses. Traditional manual plant health assessments are error-prone and inefficient for large-scale production. To address this need, we collected a comprehensive dataset covering the entire life span of tomato plants, annotated across 5 health states from 1 to 5. Our study introduces an Attention-Enhanced DS-ResNet architecture with Channel-wise attention and Grouped convolution, refined with new training techniques. Our model achieved an overall accuracy of 80.2% using 5-fold cross-validation, showcasing its robustness in precisely classifying the health states of tomato plants.

Key Words : Deep Learning, Convolutional Neural Networks, Channel-wise Attention, Depthwise Separable Convolution, Attention-Enhanced ResNet, Plant Health State Classification

요약 토마토에는 리코펜, β -카로틴 및 비타민 C와 같은 영양소가 풍부하고 세계적으로 많이 소비되는 채소 중 하나이다. 그러나 종종 생물학적 및 환경적 스트레스 요인으로 인해 수확량 손실이 발생한다. 전통적인 작물 건강 평가는 오류가 발생하기 쉽고 대규모 생산에 비효율적이다. 이러한 문제를 해결하기 위해 건강 상태에 대해 1~5로 주석을 메긴 토마토 전체 생육기간을 다루는 포괄적인 데이터 세트를 수집하였다. 우리는 Channel-wise attention과 Grouped convolution을 사용한 Attention-Enhanced DS-ResNet 아키텍처와 새로운 학습 기법을 제안한다. 우리의 모델은 5-fold 교차 검증을 사용하여 전체 정확도 80.2%를 달성하여 작물의 건강 상태를 정확하게 분류하는데 있어 견고성을 보여주었다.

주제어 : 딥러닝, 합성곱 신경망, 채널 어텐션, 깊이 분리 합성곱, Attention-Enhanced ResNet, 작물 건강 상태 분류

본 결과물은 농림축산식품부 및 과학기술정보통신부, 농촌진흥청의 재원으로 농림식품기술기획평가원과 재단법인 스마트팜연구개발사업단의 스마트팜다부처패키지혁신기술개발사업의 지원을 받아 연구되었음 (RS-2021-IP421005).

*교신저자 : Alvaro Fuentes(afuentes@jbnu.ac.kr)

접수일 2024년 06월 28일 수정일 2024년 07월 22일 심사완료일 2024년 08월 16일

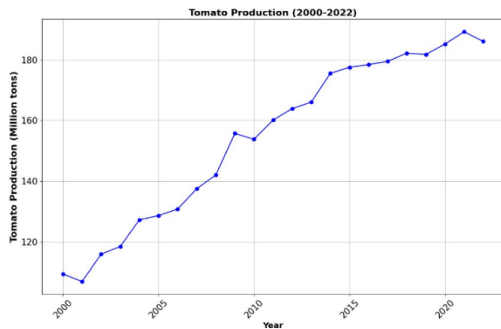


[Fig. 1] Global Tomato Production Trends Across Years [4].

1. INTRODUCTION

Tomatoes have become a significant economic crop due to their rich nutrient profile, including lycopene, β -carotene, and vitamin C [1]. Their popularity as a food staple is on the rise, making it one of the most consumed vegetables globally, ranking just below potatoes and ahead of onions [2]. Two decades ago, Europe and the Americas were the primary tomato producers, but today, Asia has taken the lead in the market [3]. Globally, tomato production has shown consistent growth over the years, as indicated by data from the Food and Agriculture Organization (FAO) [4] as shown in Fig. 1.

However, this growth is not without its challenges. Tomato plants remain vulnerable to various stressors, both biotic and abiotic. Biotic stress stems from insects, pests, and diseases, while abiotic stress includes factors such as extreme temperatures and nutrient deficiencies [5]. These challenges not only result in annual economic losses within the agricultural sector but also pose significant risks to global food security [5]. Addressing these challenges necessitates effective plant health assessment strategies.

Traditionally, such plant health assessments have relied on manual observations by pathologists. These methods involve labor-intensive visual inspection of plant symptoms and physical examination of plant tissues. While thorough, such methods are characterized by their significant time and effort requirements, making them impractical for large-scale agricultural operations [6]. Additionally, because these assessments are based on human judgment, they are inherently subjective and prone to variability and errors. The extensive labor and time needed for manual evaluations further limit their scalability, hindering their application in large fields. Consequently, there is an urgent need for innovative approaches that can provide accurate, scalable, and efficient evaluations of tomato plant health.

In recent years, the integration of deep learning techniques into agriculture has presented a promising solution. A key advantage of deep learning is its capability to directly utilize raw data without relying on manually crafted features [7]. Previous studies have showcased deep learning's potential in disease identification across various plant species, including apples [8], papaya [9], tomatoes [10], [11], paprika [12], rice [13], potatoes [14], and carrots [15].

Despite this progress, significant gaps remain in leveraging deep learning for accurately determining the true health state of plants. Much of the existing literature primarily focuses on classifying diseases or enhancing detection performance, rather than providing insights into the overall health condition of plants.

To address this gap, we undertook the development of a comprehensive dataset that covers the entire lifespan of tomato plants. These images were then meticulously annotated by domain experts into five distinct health states, ranging from 1 to 5, where 1 represents severely unhealthy and 5 denotes excellent health. This meticulous classification allows for precise categorization of plant health, offering farmers

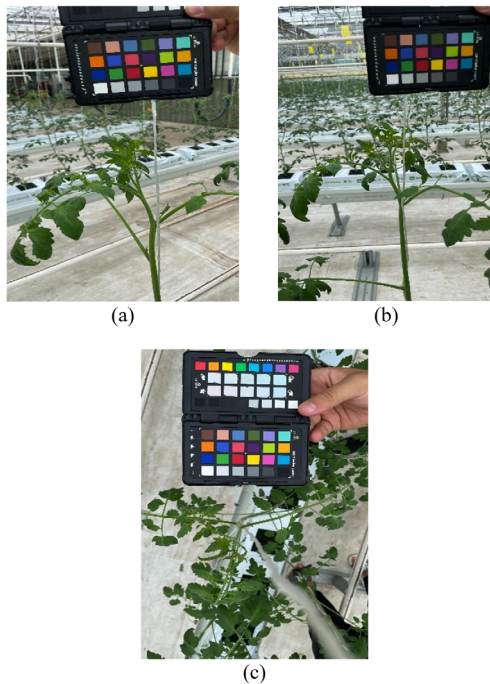


[Fig. 2] Example of Plant 10 during Week 3:
(a) Right View, (b) Left View, and (c) Top View.

invaluable insights to make informed decisions and implement targeted interventions tailored to the specific health state of their crops.

The objective of the current study is to introduce deep learning as an approach for assessing the health of tomato plants. This study presents three primary contributions to the field of plant health assessment.

1) Development of a Comprehensive Dataset: We collected a dataset covering the entire lifespan of tomato plants. This dataset includes images of 50 monitored tomato plants spanning 25 weeks. Each week, images of every plant were captured from three distinct angles: left view, right view, and top view.

2) Attention-Enhanced DS-ResNet: We propose the Attention-Enhanced DS-ResNet, a modified ResNet-18 architecture with Channel-wise attention and Group convolution. We incorporate several new training techniques, including the AdamW optimizer, and employ advanced data augmentation

methods such as Mixup and Cutmix, along with regularization techniques like Label Smoothing.

3) Evaluation of the Proposed Model: We evaluated the proposed model using the 5-fold cross-validation method on our tomato plant dataset. The proposed model achieved promising results in accurately determining the precise health state of the tomato plants.

2. MATERIALS AND METHODS

2.1 Dataset Description

1) Dataset Acquisition: As a first step, we obtained the experimental dataset to train our model and validate the performance of the proposed architecture. The dataset for this study was collected from the greenhouse facility in Buyeo, South Korea. It comprises images of tomato plants belonging to the *Solanum lycopersicum* var. *cerasiforme* Nonari species[1], collected throughout their entire lifespan. A total of 50 tomato plants were monitored during this period. Weekly visits to the greenhouse facility were conducted over 25 weeks. During each visit, we acquired three high-resolution RGB images for each plant, capturing them from three different angles: Right View, Left View, and Top View, as illustrated in Fig. 2. The images were taken using a cell phone camera, and each plant was labeled with a tag for identification purposes. The image acquisition spanned from August 2022 to December 2022. Our focus was on capturing images of the top part of the plant, as this section is sensitive and exhibits signs swiftly in response to environmental stress, nutritional deficits, or disease presence.

⟨Table 1⟩ presents the distribution of images per class in the experimental dataset. Notably, there's a varied distribution across the classes, with Class 4 containing the highest count at 1412 images, while Class 1 has the lowest, with only

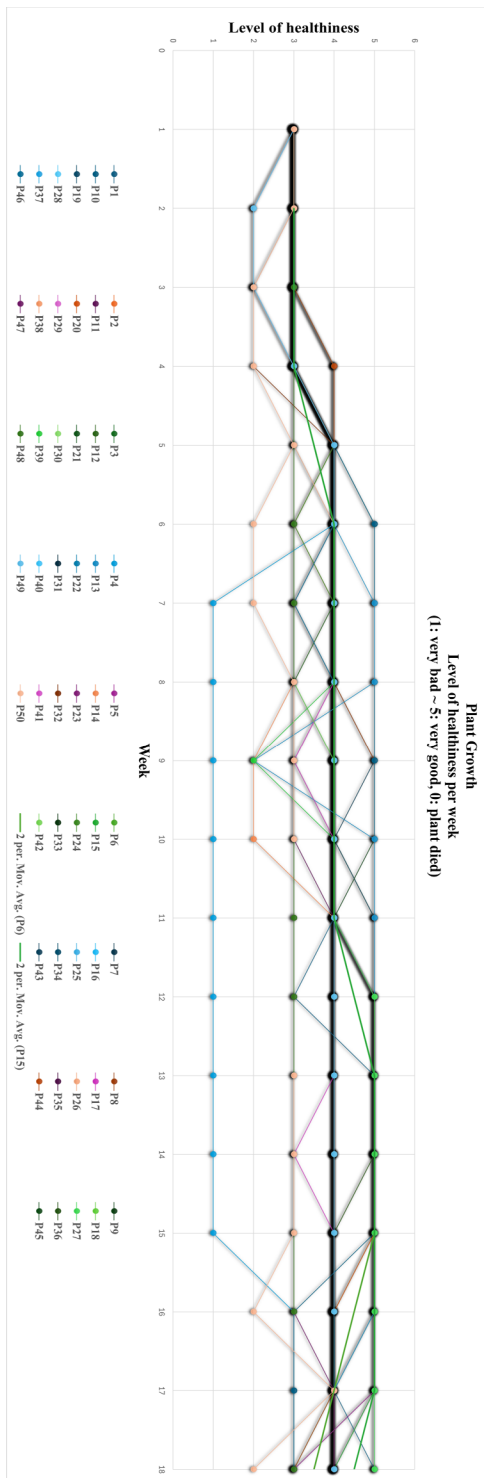


[Fig. 3] Temporal Changes of Plant Health in Cultivation Using Domain Expert Annotations.

<Table 1> Distribution of images per class in the experimental dataset.

Class	Number of Images
Class 1	18
Class 2	27
Class 3	756
Class 4	1412
Class 5	341
Total	2554

18 images. The dataset comprises a total of 2554 images.

2) Data Annotation: The dataset was meticulously annotated by domain experts, with each image assigned a health status label ranging from 1 to 5. Parameters like disease symptoms, plant morphology, growth patterns, pest infections, and nutrient deficiencies were considered. Label 5 indicated optimal health, while label 4 represented minor deviations from optimal health. Moderate health decline was labeled as 3, and severe issues were marked as 2. Images with significant health problems, like clear signs of disease, received a label of 1. This meticulous labeling ensured precise categorization, enabling comprehensive analysis of plant health across the dataset.

3) Dataset Distribution: One of the most common strategies for splitting a dataset into training and validation sets is by assigning percentages, such as 70:30 or 80:20. However, one problem that can arise with this strategy is that high validation accuracy doesn't always guarantee a robust model. When employing this division strategy, there's a risk of excluding important information from the training data, which could introduce bias into the results. Additionally, since samples for class 1 and class 2 are very few, we excluded them from this study to avoid potential biases.

Therefore, in this research, we apply a k-fold cross-validation method to evaluate the performance of the model. The k-folds method

aims to ensure that all features of the dataset are included in both the training and validation phases. We opted for a 5-fold stratified cross-validation. The dataset is divided into five subsets of approximately equal size, termed folds. Each fold serves alternately as a validation set while the remaining folds are utilized for training. This process is repeated five times, ensuring that every data point is utilized for both training and validation purposes.

4) Changes in Plant Health During Cultivation Based on Domain Expert Annotations: Fig. 3 displays the health status of all 50 plants throughout the cultivation period, based on annotations from domain experts. The horizontal axis represents weeks of data collection, while the vertical axis shows health states from 1 to 5, with 0 indicating plant death. Each point marks a plant's health at a specific week, illustrating changes over time. This visualization provides insights into changes in plant health over the entire cultivation period. From this visualization, we can see that most of the time, the health of the plants tends to be between 3 and 5, indicating a good health state. This is likely due to the plants being grown in a greenhouse environment and they receive meticulous care.

2.2 Attention-Enhanced DS-ResNet

1) SE Attention Module: To tackle the challenges posed by complex background and irrelevant factors in tomato plant images, we enhanced the ResNet-18 architecture[16] by incorporating the SE (squeeze-and-excitation) attention module [17]. The SE module is a lightweight attention mechanism designed to enhance inter-channel attention, thereby improving the model's ability to extract crucial features while reducing the influence of other interferences and enhancing recognition performance. The SE module consists of two components: squeeze and excitation. By integrating the SE module, the model learns to assign greater importance to significant features

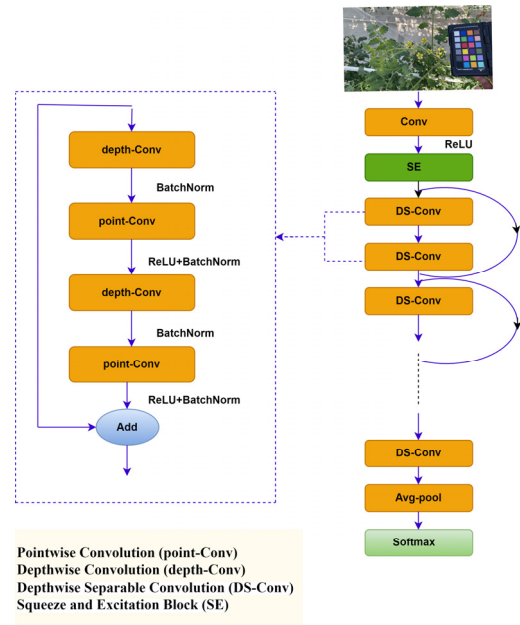


[Fig. 4] Architecture design of the proposed Attention-Enhanced DS-ResNet.

while reducing sensitivity to irrelevant features.

2) Introduction to Group Convolution: Inspired by MobileNet[18], our architecture incorporates depthwise separable convolution, a technique optimized for reducing computational complexity without compromising feature representation quality. Unlike traditional convolutional layers that apply a single set of filters to the entire input volume, depthwise convolution processes each channel independently, followed by pointwise convolution for efficient channel aggregation.

3) Detailed Architecture Overview: As illustrated in Fig. 4, Our model begins with a standard convolution layer, followed by a SE layer to adjust channel importance. The output then flows through seven residual blocks, each containing two depthwise separable convolution (DS-Conv) layers with 64 channels. An additional non-residual DS-Conv layer is included before the final layers, totaling 15 DS-Conv layers. Dilations (d_w , d_h) in these layers expand the receptive field, increasing as $2 \lfloor \frac{i}{3} \rfloor$ for the i th layer. The model concludes with an average-pooling layer followed by a fully

〈Table 2〉 Training configuration parameters.

Training Parameter	Setting
Optimization Method	AdamW
Loss Function	Categorical Cross Entropy
Regularization Scheme	Label Smoothing (0.1)
Learning Rate Scheduler	Cosine Decay
Activation Function	GeLU
Early Stopping Patience	20 epochs
Optimizer Momentum (β_1, β_2)	0.9, 0.999
Weight Decay	8×10^{-2}

connected softmax layer and has around 72K parameters.

2.3 Implementation

We developed our experimental framework using Python 3.8 and PyTorch deep learning library version 1.10.1, running on an NVIDIA GeForce RTX 3090 GPU with 24,268 MB of memory. To ensure robust model evaluation, we employed a stratified 5-fold cross-validation strategy. This involved partitioning the dataset into five folds with balanced class distributions, facilitating comprehensive training and testing cycles. Each model iteration was trained on four folds while validating on the fifth fold. This process was repeated five times to ensure the reliability of the results. During training, we implemented early stopping to mitigate overfitting, terminating training when performance on the validation set plateaued. We utilized a batch size of 32 to optimize training efficiency and storage limitation. To overcome dataset limitations and class imbalances, various data augmentation techniques were applied, including geometric transforms (rotation, horizontal flip), color variations (brightness, contrast, saturation), CutMix, and Mixup. All images were resized to 224x224 pixels to match the model's input requirements. Data preprocessing involved normalizing the input images with mean values of [0.485, 0.456, 0.406] and standard deviations of [0.229, 0.224, 0.225].

This normalization procedure centered the pixel values around zero and standardized their deviations close to one. Such normalization enhances training stability and promotes the convergence of optimization algorithms. For model optimization, we utilized the AdamW algorithm with a learning rate of 3×10^{-6} . Additionally, a cosine decay learning rate scheduler was implemented to improve training dynamics and avoid local minima. The models were trained for a total duration of 12 hours and 25 minutes.

〈Table 2〉 presents the training configuration parameters used in our experiments. These parameters were carefully selected to optimize the training process and enhance the performance of the model.

2.4 Evaluation Metrics

To assess our model's performance, we considered four key evaluation metrics. The first metric to evaluate was accuracy, which is determined by the model's overall performance across all classes by comparing the number of correct predictions to the total predictions made, as indicated by (1). Precision, our second metric, reflects the model's accuracy in identifying positive samples by dividing the number of correctly classified positive samples by the total samples classified as positive, determined by (2). Recall, also known as sensitivity, measures the ability of the model to correctly identify positive instances from the total actual positives. It's determined by dividing the number of true positive predictions by the total number of actual positive instances, as specified by (3). Finally, we analyzed the F1 score parameter. The F1 score is the harmonic mean of precision and recall. It provides a single score that balances both precision and recall, as determined by (4).

$$\text{Accuracy} = (\text{TP} + \text{TN}) / (\text{TP} + \text{FP} + \text{FN} + \text{TN}) \quad (1)$$

$$\text{Precision} = \text{TP} / (\text{TP} + \text{FP}) \quad (2)$$

$$\text{Recall} = \text{TP} / (\text{TP} + \text{FN}) \quad (3)$$

⟨Table 3⟩ Cross-validation results.

Fold	Precision	Recall	F1 Score	Validation Accuracy
1	0.83	0.81	0.82	0.82
2	0.81	0.81	0.82	0.82
3	0.79	0.76	0.78	0.78
4	0.77	0.76	0.77	0.79
5	0.81	0.79	0.80	0.80
Mean	0.802	0.786	0.798	0.802

$$F1\text{-Score} = 2 \times (P \times R) / (P + R) \quad (4)$$

Where TP denotes True Positive, TN stands for True Negative, FP indicates False Positive, and FN signifies False Negative.

3. RESULTS AND DISCUSSION

In this section, we examine the evaluation results of our proposed Attention-Enhanced DS-ResNet architecture model for classifying plant health states using our tomato plant health dataset.

⟨Table 3⟩ presents the validation accuracy, F1 score, precision, and recall obtained using the 5-fold cross-validation approach to evaluate our model's performance. These results indicate that our model maintains an overall accuracy of 80.2%, precision of 80.2%, recall of 78.6%, and an F1 score of 79.8% across all five folds. The model performs consistently across all folds during both training and validation phases, suggesting good generalization.

Fig. 5 presents the model's performance during both training and validation stages for assessing plant health. This figure provides insights into the model's learning trajectory over epochs. As the training progresses through epochs, we observe improvements in both the training and validation accuracies, along with decreases in training and validation losses. This suggests that the model's predictive performance improves not only on the training data but also on new, unseen data. Furthermore, the duration of training varied across different folds of the dataset. Fold 1 underwent training for 150 epochs, and Fold 2 concluded after 101 epochs.



[Fig. 5] Learning curves for Fold 1 of our model's training and validation phases.

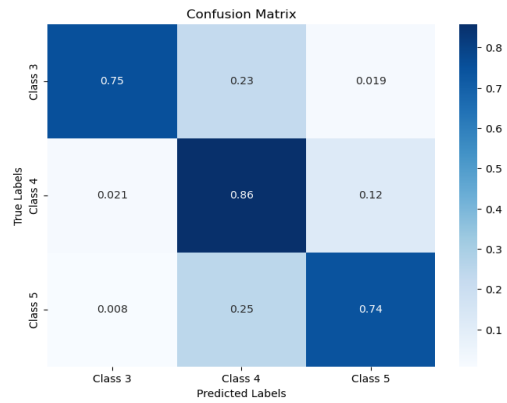


[Fig. 6] Confusion matrix for our model's performance on the validation data.

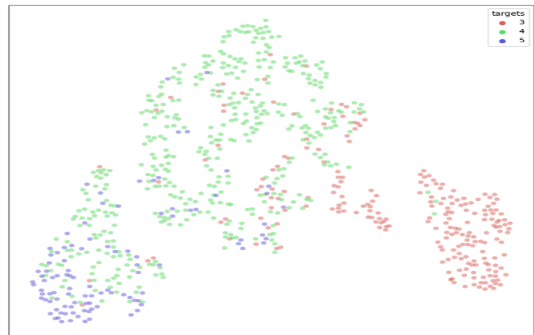


[Fig. 7] t-SNE Visualization with Validation Data and Model Weights from Fold 1

Fold 3 completed training in 81 epochs, Fold 4 terminated after 101 epochs, and Fold 5 completed its training after 133 epochs.

The confusion matrix depicted in Fig. 6 provides a comprehensive evaluation of our model's performance in classifying plant health.

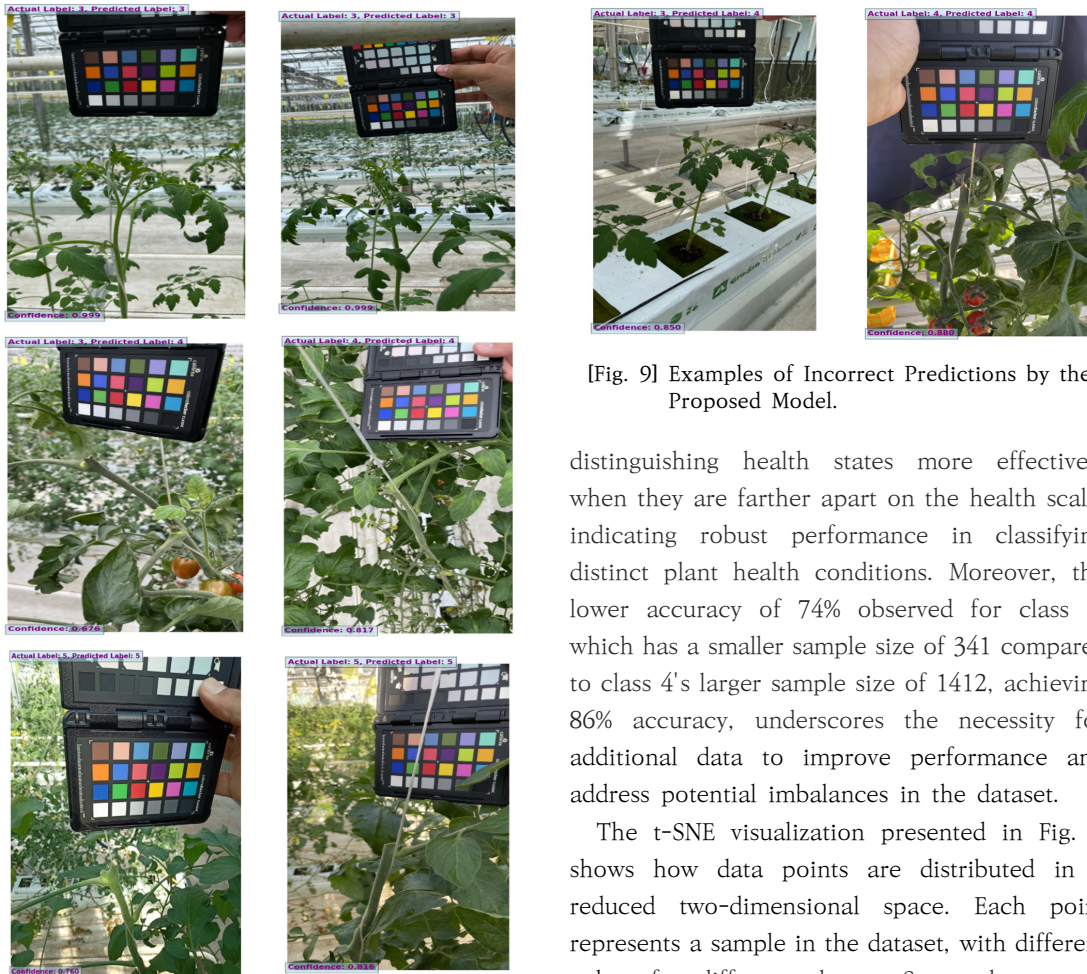


[Fig. 8] Exemplars of Predicted Images by the Proposed Model.

We observe high values along the diagonal, indicating accurate predictions: 75% for class 3, 86% for class 4, and 74% for class 5. However, instances of confusion between closely related adjacent classes are notable; for example, class 3 is misclassified as class 4 with a 23% probability and class 5 as class 4 with a 25% probability. This observation highlights the challenges in accurately differentiating between adjacent health states due to overlapping characteristics and complexities within the dataset. Importantly, minimal confusion is observed between class 3 and class 5 as they are not adjacent on the health assessment scale. This suggests the model's proficiency in



[Fig. 9] Examples of Incorrect Predictions by the Proposed Model.

distinguishing health states more effectively when they are farther apart on the health scale, indicating robust performance in classifying distinct plant health conditions. Moreover, the lower accuracy of 74% observed for class 5, which has a smaller sample size of 341 compared to class 4's larger sample size of 1412, achieving 86% accuracy, underscores the necessity for additional data to improve performance and address potential imbalances in the dataset.

The t-SNE visualization presented in Fig. 7 shows how data points are distributed in a reduced two-dimensional space. Each point represents a sample in the dataset, with different colors for different classes. Some classes mix together, while others form distinct clusters. Classes 4 and 5 overlap significantly, indicating that they share similar features. This overlap occurs because the health states are arranged in order from 1 (poor health) to 5 (optimal health), and neighboring classes tend to have similar characteristics. For example, both classes 4 and 5 represent healthy plants, so the model might get confused between these neighboring classes due to their subtle differences. In contrast, classes 3 and 5, which are not adjacent to each other, are more clearly separated. The overlap between adjacent classes decreases when there is sufficient training data available, as observed between classes 3 and 4. This highlights the need for adequate training data for all classes, enabling

(Table 4) Comparison with baseline model Resnet18 and Attention-Enhanced DS-Resnet.

Model	Precision	Recall	F1 Score	Validation Accuracy
Attention-Enhanced DS-ResNet	0.802	0.786	0.798	0.802
ResNet 18	0.760	0.710	0.730	0.800

the model to better differentiate between classes.

The proposed model's architecture and weights were saved for each fold of the data. During the prediction phase, we employed the validation data from fold 2 along with the corresponding stored model weights. For each prediction, the image, the true result, and the result of the prediction made with the proposed model were displayed, together with the percentage of accuracy. Fig. 8 illustrates several prediction outcomes from the model, highlighting its high confidence in accurate predictions. However, we observed some instances of incorrect predictions. In the first image of Fig. 9, the presence of multiple plants complicates the model's focus, leading to an incorrect prediction. In the second image of Fig. 9, despite assigning label 5 to the plant due to pruning, its poor appearance caused the model to predict label 4.

Fig. 10 shows the class-wise performance of the Attention-Enhanced DS-ResNet and ResNet models across three metrics: precision, recall, and F1 score. The Attention-Enhanced DS-ResNet generally achieves higher scores across these metrics compared to ResNet. Additionally, the lower performance for Class 5 compared to Classes 3 and 4 is likely due to the smaller sample size of Class 5, which leads to less training data and reduced performance.

(Table 4) presents a comparative analysis between our modified model, Attention-Enhanced DS-ResNet, and the baseline ResNet18. Our model demonstrates superior performance across key metrics, including precision, recall, F1 score, indicating its effectiveness in reducing false negatives and false positives. It also shows a slight improvement in validation accuracy

over ResNet18. This highlights how channel-wise attention and grouped convolutions not only enhance performance but also reduce computational costs due to the efficiency of grouped convolutions.

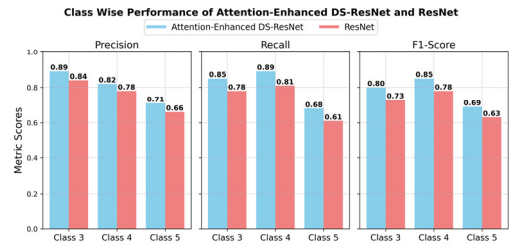


[Fig. 10] Class-wise performance of Attention-Enhanced DS-ResNet (sky blue) and ResNet (light coral) for Precision, Recall, and F1-Score. Values on the bars represent metric scores for each class (Class 3, Class 4, Class 5).

4. CONCLUSION

In this study, we developed a deep learning-based approach to accurately determine the health state of tomato plants. Our proposed method, Attention-Enhanced DS-ResNet, modifies the ResNet-18 architecture by integrating Channel-wise attention and Group convolution. We collected a comprehensive dataset capturing images of tomato plants throughout their lifespan, which serves as a valuable resource for this study. The model's performance was evaluated using 5-fold cross-validation, achieving an overall accuracy of 80.2%, with significant improvements in precision, recall, and F1 score. Our approach offers practical advantages by automating the health assessment process, reducing the need for human intervention, and enhancing efficiency. This automation benefits

farmers by enabling precise health status determinations and facilitating targeted interventions, ultimately improving crop management and yields.

REFERENCES

- [1] A. Gerszberg, K. Hnatuszko-Konka, T. Kowalczyk, and A. K. Kononowicz, "Tomato (*Solanum lycopersicum* L.) in the service of biotechnology," *Plant Cell, Tissue and Organ Culture (PCTOC)*, Vol.120, No.3, pp.881-902, 2015.
- [2] V. Bergougnoux, "The history of tomato: From domestication to biopharming," *Biotechnol Adv*, Vol.32, No.1, pp.170-189, 2014.
- [3] A. Fuentes, Y. Lee, Y. Hong, and S. Yoon, "Characteristics of Tomato Plant Diseases - A Study for Tomato Plant Disease Identification," in *ISITC 2016 International Symposium on Information Technology Convergence*, Shanghai, China, 2016.
- [4] Food and Agriculture Organization of the United Nations, "fao_website (<https://www.fao.org/faostat/en/#data/QCL>)," 2024.
- [5] M. Nawaz et al., "A review of plants strategies to resist biotic and abiotic environmental stressors," *Science of The Total Environment*, Vol.900, p.165832, 2023.
- [6] G. K. Sandhu and R. Kaur, "Plant Disease Detection Techniques: A Review," in *2019 International Conference on Automation, Computational and Technology Management (ICACTM)*, IEEE, pp.34-38, 2019.
- [7] M. Brahimi, K. Boukhalfa, and A. Moussaoui, "Deep Learning for Tomato Diseases: Classification and Symptoms Visualization," *Applied Artificial Intelligence*, Vol.31, No.4, pp.299-315, 2017.
- [8] Y. Tian, E. Li, Z. Liang, M. Tan, and X. He, "Diagnosis of Typical Apple Diseases: A Deep Learning Method Based on Multi-Scale Dense Classification Network," *Front Plant Sci*, Vol.12, Oct. 2021.
- [9] J. L. de Moraes, J. de Oliveira Neto, C. Badue, T. Oliveira-Santos, and A. F. de Souza, "Yolo-Papaya: A Papaya Fruit Disease Detector and Classifier Using CNNs and Convolutional Block Attention Modules," *Electronics (Basel)*, Vol.12, No.10, p.2202, 2023.
- [10] A. Fuentes, S. Yoon, J. Lee, and D. S. Park, "High-Performance Deep Neural Network-Based Tomato Plant Diseases and Pests Diagnosis System With Refinement Filter Bank," *Front Plant Sci*, Vol.9, 2018.
- [11] A. Guerrero-Ibañez and A. Reyes-Muñoz, "Monitoring Tomato Leaf Disease through Convolutional Neural Networks," *Electronics (Basel)*, Vol.12, No.1, p.229, 2023.
- [12] J. Dong, A. Fuentes, S. Yoon, H. Kim, and D. S. Park, "An iterative noisy annotation correction model for robust plant disease detection," *Front Plant Sci*, Vol.14, 2023.
- [13] Y. Meng, M. Xu, H. Kim, S. Yoon, Y. Jeong, and D. S. Park, "Known and unknown class recognition on plant species and diseases," *Comput Electron Agric*, Vol.215, p.108408, Dec. 2023.
- [14] F. Arshad et al., "PLDPNet: End-to-end hybrid deep learning framework for potato leaf disease prediction," *Alexandria Engineering Journal*, Vol.78, pp.406-418, 2023.
- [15] W. Xie, S. Wei, Z. Zheng, Y. Jiang, and D. Yang, "Recognition of Defective Carrots Based on Deep Learning and Transfer Learning," *Food Bioproc Tech*, Vol.14, No.7, pp.1361-1374, 2021.
- [16] K. He, X. Zhang, S. Ren, and J. Sun, "Deep Residual Learning for Image Recognition," in *2016 IEEE Conference on Computer Vision and Pattern Recognition (CVPR)*, IEEE, pp.770-778, 2016.
- [17] J. Hu, L. Shen, and G. Sun, "Squeeze-and-Excitation Networks," in *2018 IEEE/CVF Conference on Computer Vision and Pattern Recognition*, IEEE, pp.7132-7141, 2018.
- [18] A. G. Howard et al., "MobileNets: Efficient Convolutional Neural Networks for Mobile Vision Applications," *CoRR*, Vol.abs/1704.04861, 2017.

세이드 알리 에스거(Syed Ali Asgher) [준회원]



- 2020년 8월 : 인도 Islamic University of Science and Technology, 컴퓨터공학과 학사
- 2024년 8월 : 전북대학교 전자정보공학부 석사

<관심분야>

컴퓨터 비전, 인공지능

이 재 환(Jaehwan Lee)

[정회원]



- 2014년 8월 : 전북대학교 전자정보공학부 석사
- 2024년 8월 : 전북대학교 전자정보공학부 박사

<관심분야>

기계학습, 딥러닝, 컴퓨터 비전

알바로 푸엔테스(Alvaro Fuentes)

[정회원]



- 2016년 2월 : 전북대학교 전자정보공학부 석사
- 2019년 8월 : 전북대학교 전자정보공학부 박사
- 2019년 9월 ~ 2022년 8월 : 전북대학교 전자정보공학부 박사 후과정

- 2022년 9월 ~ 현재 : 전북대학교 지능형로봇연구소 연구교수

<관심분야>

기계학습, 딥러닝, 컴퓨터 비전, 로봇공학

윤 숙(Sook Yoon)

[정회원]



- 1995년 2월 : 전북대학교 정보통신학과 석사
- 2003년 2월 : 전북대학교 전자공학과 박사
- 2023년 3월 ~ 2006년 6월 : 미국 University of California, Post Doc.

- 2006년 9월 ~ 2017년 2월 : 목포대학교 멀티미디어공학과 부교수
- 2017년 2월 ~ 현재 : 목포대학교 컴퓨터공학과 교수

<관심분야>

컴퓨터 비전, 객체인식, 기계학습, 생체인식

박 동 선(Dong Sun Park)

[정회원]



- 1984년 12월 : 미국 University of Missouri Electrical and Computer Engineering 석사
- 1990년 12월 : 미국 University of Missouri Electrical and Computer Engineering 박사

- 1997년 4월 ~ 2002년 3월 : 전북대학교 전자공학 부교수
- 2002년 4월 ~ 2020년 8월 : 전북대학교 전자공학 교수
- 2020년 9월 ~ 현재 : 전북대학교 지능형로봇연구소 명예교수

<관심분야>

패턴인식, 컴퓨터 비전, 딥러닝, 인공지능망, 인공지능